CANCER DISCOVERY

Discovery of a mutant-selective covalent inhibitor of EGFR that overcomes T790M-mediated resistance in NSCLC

Annette O Walter, Robert Tjin Tham Sjin, Henry J Haringsma, et al.

Cancer Discovery Published OnlineFirst September 24, 2013.

Discovery of a mutant-selective covalent inhibitor of EGFR that overcomes T790M-mediated resistance in NSCLC

Annette O. Walter[1], Robert Tjin Tham Sjin[2], Henry J. Haringsma[1], Kadoaki Ohashi[3], Jing Sun[3], Kwangho Lee[2], Aleksander Dubrovskiy[2], Matthew Labenski[2], Zhendong Zhu[2], Zhigang Wang[2], Michael Sheets[2], Thia St Martin[2], Russell Karp[2], Dan van Kalken[2], Prasoon Chaturvedi[2], Deqiang Niu[2], Mariana Nacht[2], Russell C. Petter[2], William Westlin[2], Kevin Lin[1], Sarah Jaw-Tsai[1], Mitch Raponi[1],Terry Van Dyke[4,5], Jeff Etter[1], Zoe Weaver[5], William Pao[3], Juswinder Singh[2], Andrew D. Simmons[1], Thomas C. Harding[1*], Andrew Allen[1]

Affiliations: [1]Clovis Oncology Inc., San Francisco, CA 94158; [2]Celgene Avilomics Research, Bedford, MA 01730; [3]Department of Medicine/Division of Hematology-Oncology, Vanderbilt University School of Medicine, Nashville, TN 37232, USA [4]Mouse Cancer Genetics Program, NCI-Frederick, MD 21702; [5]Center for Advanced Preclinical Research, SAIC-Frederick, Inc., NCI-Frederick, MD 21702

Running title: Development of covalent EGFR T790M inhibitor in NSCLC

Keywords: NSCLC, EGFR, drug resistance, T790M, EMT

Financial support: This project was funded in part with federal funds from the National Cancer Institute, National Institutes of Health, under Contract No. HHSN261200800001E. The content of this publication does not necessarily reflect the views or policies of the Department of Health and Human Services, nor does mention of trade names, commercial products, or organizations imply endorsement by the U.S. Government. WP received additional funding from National

Institutes of Health (NIH) NCI grants R01CA121210, P01CA129243, U54CA143798, and P30CA68485.

Corresponding author: Thomas C. Harding, Ph.D; e-mail: tharding@clovisoncology.com; Clovis Oncology, Inc., 1700 Owens Street, Suite 205, San Francisco, CA 94158; Tel: (415) 409-5472; Fax: (415) 552-3427

Conflict of interest statement: Authors affiliated with [1]Clovis Oncology Inc., San Francisco, CA 94158 and [2]Celgene Avilomics Research, Bedford, MA 01730 received financial and stock option incentives from a publically traded company (Clovis Oncology Inc. and Celgene, respectively).

Word count (excluding references): 5,858

Total number of figures and tables: 7 (5 figures; 2 tables)

ABSTRACT (153 of 150 words max.)

Non-small cell lung cancer (NSCLC) patients with activating epidermal growth factor receptor (EGFR) mutations initially respond to first generation reversible EGFR tyrosine kinase inhibitors. However, clinical efficacy is limited by acquired resistance, frequently driven by the EGFR T790M mutation. CO-1686 is a novel, irreversible and orally delivered kinase inhibitor that specifically targets the mutant forms of EGFR including T790M while exhibiting minimal activity towards the wild-type (WT) receptor. Oral administration of CO-1686 as single agent induces tumor regression in EGFR mutated NSCLC tumor xenograft and transgenic models. Minimal activity of CO-1686 against the WT EGFR receptor was observed. In NSCLC cells with acquired resistance to CO-1686 *in vitro*, there was no evidence of additional mutations or amplification of the *EGFR* gene, but resistant cells exhibited signs of epithelial-mesenchymal transition (EMT) and demonstrated increased sensitivity to AKT inhibitors. These results suggest CO-1686 may offer a novel therapeutic option for patients with mutant EGFR NSCLC.

STATEMENT OF SIGNFICANCE

We report the preclinical development of a novel covalent inhibitor, CO-1686, that irreversibly and selectively inhibits mutant EGFR, in particular the T790M drug-resistance mutation, in NSCLC models. CO-1686 is the first drug of its class in clinical development for the treatment of T790M-positive NSCLC, potentially offering potent inhibition of mutant EGFR while avoiding the on-target toxicity observed with inhibition of the wild-type EGFR receptor.

INTRODUCTION

Despite years of research and prevention strategies, lung cancer remains the most common cancer worldwide with approximately 1.35 million new cases annually. Non-small cell lung cancer (NSCLC) accounts for almost 85% of all lung cancers (1). Additionally, lung cancer continues to be the most common cause of cancer-related deaths worldwide with a 5-year survival rate of less than 20% in patients in the US (http://seer.cancer.gov).

Activating mutations in the epidermal growth factor receptor (EGFR) are key drivers of NSCLC malignancy in 10-15% of patients of European descent and approximately 30% of patients of East Asian descent (2). Patients with the most common EGFR mutations (L858R mutation in exon 21 and delE746-A750 deletions in exon 19) typically have good responses to therapy with first-generation reversible EGFR tyrosine kinase inhibitors (TKIs), such as erlotinib or gefitinib (3-5). Toxicity associated with both erlotinib and gefitinib includes skin rash and diarrhea related to inhibition of wild-type EGFR (WT EGFR) in skin and intestine, respectively (6).

Despite the impressive initial response to treatment, disease progression generally occurs after 9 to 14 months of erlotinib or gefitinib therapy, driven in approximately 60% of cases by a second site EGFR point mutation that results in the substitution of threonine with methionine at amino acid position 790 (T790M;(7-10)). Research suggests that T790M mediates resistance to first-generation EGFR inhibitors by acting as a "gatekeeper" mutation, inducing steric hindrance in the ATP-binding pocket and preventing inhibitor binding (8, 11, 12). Additional work has indicated that T790M increases the affinity of EGFR for ATP, therefore out-competing ATP-competitive TKIs and restoring enzymatic activity in their presence (13).

Patients with mutant EGFR NSCLC who have failed treatment with first generation EGFR TKIs and have acquired resistance through the T790M mutation have few treatment options. There are no targeted therapies for these patients, who are currently treated with cytotoxic chemotherapy that has limited efficacy, but significant toxicity, in the second- or third-line setting. Although second generation irreversible HER-family TKIs, including dacomitinib (PF299804) and afatinib (BIBW2992), are able to inhibit T790M-mutant EGFR *in vitro*, in clinical trials these agents have not been shown to induce compelling responses in patients that have failed first-generation TKIs (14). Likely due to the potent inhibition of WT EGFR and its consequent toxicities, these agents cannot reach exposures in the clinic required to inhibit T790M in tumor tissue. To circumvent this problem, a covalent inhibitor that inhibits mutant EGFR, including T790M, more potently than the WT receptor, termed WZ4002, was described (15), but did not progress into human clinical trials. Recently PKC-412 (midostaurin), an indolocarbazole compound currently in development as a FLT-3 inhibitor in acute myeloid leukemia, was described to selectively inhibit T790M over WT EGFR in a non-covalent fashion (16). As a staurosporine-derived compound, PKC412 has a broad kinase inhibition profile (17) and its clinical application in T790M positive NSCLC is therefore questionable, particularly since it doesn't potently inhibit activating EGFR mutations. Hence, there is currently a need for an EGFR-TKI that is able to effectively treat T790M-positive lung tumors.

In the current study, we report the preclinical validation of a 2,4-disubstituted pyrimidine compound, CO-1686, that irreversibly and selectively inhibits mutant EGFR, in particular the T790M drug-resistance mutation, in NSCLC models. Oral administration of CO-1686 leads to tumor regressions in cell-based and patient-derived xenograft models as well as in a transgenic mouse model expressing mutant forms of human EGFR. In these models, acquired resistance to

this third generation EGFR TKI is not mediated by further second-site mutations or amplification of the *EGFR* gene and resistant cells appear to have a reduced dependence on EGFR signaling compared to parental cells. CO-1686 is currently being evaluated in phase I/II clinical trials in EGFR-mutant NSCLC.

RESULTS

CO-1686 is a potent and irreversible inhibitor of EGFR *in vitro*. Using a structure-based approach, we designed and developed a potent 2,4-disubstituted pyrimidine molecule, CO-1686, that covalently modified the conserved Cys797 in the ATP binding pocket of the EGFR kinase domain (Fig. 1A). As shown in the structural model of CO-1686 in complex with EGFR T790M, the *meta* acrylamide points to Cys797 and forms the covalent bond (Fig. 1B). To confirm that CO-1686 covalently modified the EGFR L858R/T790M kinase we performed mass spectrometry. Incubation of CO-1686 with recombinant EGFR L858R/T790M protein resulted in a mass shift of EGFR L858R/T790M consistent with the formation of a covalent complex between CO-1686 and the EGFR L858R/T790M protein (SI Fig. 1A). Pepsin digest analyses confirmed that CO-1686 modified the conserved Cys797 residue in the EGFR L858R/T790M kinase domain (SI Fig. 1B, C).

To determine the selectivity and potency of CO-1686 *in vitro* we performed kinetic studies using recombinant WT EGFR and mutant EGFR L858R/T790M kinases. When assessing a covalent inhibitor like CO-1686, potency is expressed by using the ratio (k_{inact}/K_i) of the inactivation rate constant (k_{inact}) with respect to the binding constant (K_i) since the amount of active EGFR enzyme changes over time. CO-1686 is a potent inhibitor of EGFR L858R/T790M kinase (k_{inact}/K_i = (2.41 ± 0.30) x 10^5 $M^{-1}s^{-1}$) and is approximately 22-fold selective over WT EGFR (k_{inactt}/K_i = (1.12 ± 0.14) x 10^4 $M^{-1}s^{-1}$) (Table 1). As expected for a first generation TKI, erlotinib potently inhibited WT EGFR (K_i = 0.40 ± 0.03 nM) while it had little activity against EGFR L858R/T790M kinase (K_i = 98.0 ± 8.1 nM). CO-1686 also demonstrated a favorable selectivity profile when profiled against 434 kinases (SI Table 1A). Twenty-three targets (representing 14 different kinases) were identified to be inhibited >50% at 0.1 μM CO-1686.

EGFR del19, T790M, L858R/T790M and L858R mutant kinases demonstrated the highest degree of inhibition, indicating the specificity of CO-1686, however, other kinase targets were observed to be inhibited at lower potency including FAK, CHK2, ERBB4 and JAK3. Specificity was also examined by apparent IC_{50} determination in kinases known to possess a cysteine equivalent to C797 in EGFR (SI Table 1B). In comparison to EGFR T790M, other C797-related kinases are observed to be inhibited by CO-1686 with an IC_{50} >6-fold including members of the Tec-family and JAK3. In summary, CO-1686 is the first EGFR inhibitor in clinical development that is mutant-selective and inhibits T790M more potently than WT EGFR.

CO-1686 potently and selectively inhibits growth of NSCLC cells expressing mutant EGFR and induces apoptosis. Selectivity and activity of CO-1686 against cells expressing EGFR mutations was demonstrated in a panel of cell lines (Fig. 2A and SI Table 2). The effect of CO-1686 treatment on cell growth was determined in 4 NSCLC cell lines expressing mutant EGFR (HCC827, PC9, HCC827-EPR and NCI-H1975) and in 3 cell lines expressing WT EGFR (A431, NCI-H1299 and NCI-H358). HCC827 and PC9 cell lines both harbor the EGFR delE746-A750 activating mutation in exon 19. HCC827-EPR is a resistant clone of HCC827 that acquired T790M in response to continuous exposure to erlotinib and the MET inhibitor PHA-665,752 (18). NCI-H1975 is another T790M-positive cell line that harbors the EGFR L858R/T790M double mutation. CO-1686 potently inhibited proliferation in the mutant-EGFR NSCLC cells with GI_{50} values ranging from 7 – 32 nM. In comparison, the GI_{50} value for A431 cells, an epidermoid cell line that is driven by amplified WT *EGFR*(19), was 547 nM. Two cell lines expressing WT EGFR in the presence of an N- or KRAS mutation (NCI-H1299 and NCI-H358, respectively) were inhibited by CO-1686 at a concentration of 4275 and 1806 nM, respectively.

Similar results were obtained when determining effects of CO-1686 on EGFR signaling by immunoblot analysis in the WT-driven A431 cells compared to the EGFR mutant cells. IC_{50} values for inhibition of EGFR phosphorylation were above 2000 nM in the three WT EGFR expressing cells, while CO-1686 inhibited p-EGFR with IC_{50} values ranging from 62 – 187 nM in the mutant-EGFR expressing cells (SI Table 2) confirming the mutant-selective properties of CO-1686. CO-1686 inhibits cell proliferation and EGFR phosphorylation equally in the parental HCC827 (EGFR del19) as well as the erlotinib-resistant HCC827-EPR (del19/T790M) clone. Treatment with CO-1686 induces apoptosis in both cell lines as demonstrated by an increase in cleaved PARP and BimEL protein (Fig. 2B), irrespective of the T790M status. Erlotinib on the other hand has no effect in the T790M-positive HCC827-EPR cells (Fig. 2B). Additionally, we treated PC-9/ER (del19/T790M) and H3255/XLR cells (L858R/T790M) with erlotinib and CO-1686 in standard growth inhibition assays. Both are polyclonal populations of cells that acquired T790M in response to continuous exposure to EGFR TKIs (20). Again, CO-1686 was superior to erlotinib in inhibiting the growth of these cells (SI Fig. 2A, B). Collectively, the EGFR signaling and cell growth/apoptosis data indicate that CO-1686 selectively and potently affects cells harboring activating EGFR mutations as well as the T790M resistance mutation and has minimal activity in cells expressing WT EGFR.

CO-1686 has activity against minor EGFR mutants *in vitro*. We examined the effect of CO-1686 against other EGFR mutations occasionally found in lung cancer, such as G719S, an exon 19 insertion mutant (ex19ins: I744-K745insKIPVAI), an exon 20 insertion (ex20ins: H773-V774HVdup), and L861Q in surrogate kinase assays. All of these except the exon 20 insertion have been associated with sensitivity to first-generation EGFR TKIs (21). Similar to erlotinib,

CO-1686 was active against G719S, the exon 19 insertion, and L861Q, but not against the exon 20 insertion (SI Fig. 3).

CO-1686 demonstrates anti-tumor activity in NSCLC EGFR mutant xenograft models.

Initial CO-1686 pharmacokinetics were evaluated in female NCRnu.nu mice (n=3/gp) following IV and oral delivery (SI Fig. 4A, B). CO-1686 displayed high oral bioavailability (65%) and a relatively long half-life of 2.6 hours when dosed at 20 mg/kg. Tumor-bearing mice were dosed orally once daily with CO-1686 as single agent and its effect on tumor growth was determined in several EGFR dependent xenograft models (Fig. 3A-C). Continuous oral dosing of CO-1686 causes dose-dependent and significant tumor growth inhibition in all *EGFR*-mutant models examined. At 100 mg/kg/day CO-1686 caused tumor regressions in two erlotinib-resistant models expressing the L858R/T790M EGFR mutation, the NCI-H1975 cell line xenograft (Fig. 3A) and the patient-derived lung tumor xenograft (PDX) LUM1868 (Fig. 3B), while erlotinib had no inhibitory effect on tumor growth (Fig. 3A, B). The second generation EGFR TKI afatinib reduced tumor growth in NCI-H1975 EGFR T790M xenograft model (Fig. 3A) but to a lesser extent than observed with CO-1686 ($P < 0.01$). Anti-tumor activity of CO-1686 in the HCC827 xenograft model that expresses the exon del19 activating EGFR mutation was comparable to erlotinib and afatinib (Fig. 3C). Exploration of different oral dosing schedules demonstrated that in the NCI-H1975 model CO-1686 caused tumor regressions either given as 100 mg/kg once daily (QD) or as 50 mg/kg twice daily (BID), with no significant alterations in body weight with either dosing schedule (SI Fig. 5A, B). However, the BID CO-1686 administration schedule was statistically superior to QD day 15 post-dosing ($P < 0.01$) and was therefore chosen as the optimal dosing regimen (SI Fig. 5A).

CO-1686 is WT EGFR sparing *in vivo*. To demonstrate the mutant selectivity and wild-type sparing properties of CO-1686 *in vivo*, CO-1686 potency was evaluated in the A431 xenograft model which has been previously shown to be dependent on WT EGFR for proliferation (19, 22). In this model CO-1686 dosed at 50 mg/kg BID was compared to erlotinib and afatinib at their respective highest tolerated dose in mice (75 mg/kg QD PO and 20 mg/kg QD intraperitoneally (IP), respectively). CO-1686 exhibited a minimal (36% TGI) although significant ($P < 0.01$) reduction in tumor growth, while both erlotinib and afatinib administration resulted in tumor regression (Fig. 3D). A431 tumor lysates from animals in each treatment group were analyzed for phosphorylated WT EGFR at tyrosine 1068 (a known marker for EGFR activation; Fig. 4A, B). Compared to the vehicle control group, A431 tumors harvested from animals treated with 50 mg/kg BID CO-1686 had no detectable reductions in EGFR phosphorylation (84% phosphorylated EGFR relative to vehicle; $P = 0.58$; Fig. 4B). In contrast, A431 tumors harvested from animals treated with 75 mg/kg QD erlotinib and 20 mg/kg QD afatinib had statistically significant reductions in EGFR phosphorylation (12% and 2% phosphorylated EGFR relative to vehicle, respectively; $P < 0.05$ in both cases; Fig. 4A, B). In addition, consistent with a lack of WT EGFR inhibition, CO-1686 administration did not cause significant mouse body weight changes in the A431 xenograft experiment (SI Fig. 6). Body-weight loss was observed in both erlotinib and afatinib-treated groups ($P < 0.01$).

Sparing of WT EGFR downstream signaling by CO-1686 was also examined in mouse skin (Fig. 4C). Administration of CO-1686 at the efficacious dose of 100 mg/kg QD for 5 days had no effect on phospho-MAPK levels in normal mouse skin, while erlotinib and afatinib both inhibited MAPK phosphorylation (Fig. 4C).

These results demonstrate that CO-1686, contrary to first and second generation TKIs, spares WT EGFR *in vivo* at efficacious exposures that cause significant growth inhibition of tumors harboring mutant EGFR, including T790M.

CO-1686 demonstrates anti-tumor activity in human EGFR-L858R and EGFR-L858R-T790M expressing transgenic mice. The efficacy of CO-1686 was examined in the bitransgenic EGFR-L858R;CCSP-rtTA genetically engineered mouse (GEM) model that develops lung adenocarcinoma upon human mutant EGFR transgene induction (23). Expression of mutant human EGFR L858R was induced in GEM mice by doxycyline feeding and tumor development monitored in animals using magnetic resonance imaging (MRI) of the lungs. In this model, diffuse adenocarcinoma dependent on human EGFR L858R expression develops over the course of several weeks of induction. Four weeks post-induction, baseline MRI showed that neoplasms had developed in the lungs and animals were randomized to vehicle, CO-1686 or erlotinib treatment. Twenty-one days post-treatment initiation, animals underwent MRI to observe the impact of drug administration on tumor volume. Representative examples of post-treatment MRI scans are shown in Fig. 4D. Tumor regression was observed in 11/11 of mice treated with erlotinib at 50 mg/kg QD PO and 14/14 mice treated with CO-1686 50 mg/kg BID PO after 21-days of dosing, whereas tumor progression was recorded in all mice of the vehicle-treated group.

The efficacy of CO-1686 was also examined in the bitransgenic EGFR-L858R-T790M;CCSP-rtTA model that mimics T790M mediated acquired resistance to erlotinib and gefitinib (24). Tumor bearing animals were randomized and treated with vehicle, 50mg/kg BID CO-1686 or 20mg/kg QD afatinib. Twenty-one days post-treatment initiation, animals underwent

MRI to observe the impact of drug administration on tumor volume. Representative examples of post-treatment MRI scans are shown in Fig. 4E. The mean tumor volumes of mice in the vehicle, afatinib and CO-1686 groups were 780, 486 and 7 mm^3, respectively. Complete or near complete responses were thus observed in all mice treated with CO-1686. Immunohistochemical analysis performed on lung tumor sections from vehicle and CO-1686 treated animals confirmed that treatment with CO-1686 greatly reduced both tumor burden and cell proliferation (H&E and Ki67 staining; SI Fig. 7) in the transgenic models. Taken together, CO-1686 exhibits potent anti-tumor activity as a single agent in transgenic models with one of the most common primary human EGFR mutations (L858R), as well as the most common EGFR mutation associated with acquired resistance (L858R/T790M). These data suggest that CO-1686 may have utility in both front-line and previously treated EGFR mutant NSCLC patients.

Acquired resistance to CO-1686 is associated with EMT in T790M-positive NCI-H1975 cells. To address acquired resistance to this novel third generation mutant-selective EGFR TKI, we continuously exposed NCI-H1975 cells harboring the L858R/T790M mutation for several months to increasing doses of CO-1686 until resistance developed. We isolated five independent CO-1686 resistant (COR) clones, designated as COR 1-1, COR 1-2, COR 10-1, COR 10-2 and COR 10-3. Cell viability was determined for all clones after treatment with a first, second and third generation EGFR TKI (erlotinib, afatinib and CO-1686, respectively) and all CORs exhibited resistance to all 3 types of inhibitors, while the parental cell line was only resistant to erlotinib (Table 2). The resistance phenotype was maintained for at least 3 months in the absence of CO-1686 treatment as determined by cell viability assays (data not shown). Comparing the cell morphology of COR cell clones with the parental NCI-H1975 cells, the resistant cells

appeared to acquire a spindle-like morphology (SI Fig. 8A). The mutational status of 19 common oncogenes including *EGFR* was analyzed in resistant clones using OncoCarta v1.0 (Sequenom). No additional mutations in *EGFR* or any of the other oncogenes tested, including *MET, BRAF, ERBB2, HRAS, NRAS, KRAS* or *PIK3CA* were identified. However the original L858R/T790M mutation was present in all five clones (data not shown).

To determine if CO-1686 resistance in the COR cell clones was dependent on EGFR signaling, we examined the functional effects of *EGFR* knockdown in the NCI-H1975 parental cells as well as two representative CO-1686 resistant clones, COR 1-1 and COR 10-1, using siRNA. *EGFR* knockdown was demonstrated at the mRNA level by RT-PCR (SI Fig. 8B) as well as at the protein level by EGFR immunoblot analysis (Fig. 5A). Compared to the parental NCI-H1975 cell line, the COR cell clones demonstrated a reduced dependence on EGFR expression for viability (Fig. 5B). Averaged across the two EGFR siRNAs examined, viability was reduced 48, 15 and 4 % for NCI-H1975, COR1-1 and COR10-1, respectively, following siRNA knockdown of *EGFR*. Therefore acquired resistance to the third generation TKI CO-1686 reduces the dependence on EGFR signaling for cell viability.

To elucidate the mechanism of CO-1686 resistance, we performed RNA expression analysis of the NCI-H1975 parental and COR 1-1 and COR 10-1 cell clones using RNA-Seq. Analysis of genes significantly differentially expressed in the CO-1686 resistant cell clones compared to the parental cell line using gene set enrichment analysis (MSigDB; Broad institute) and KEGG pathway analysis (Kanehisa Laboratories; Kyoto University) demonstrated a significant enrichment of genes involved in epithelial-mesenchymal transition (EMT) in COR1-1 and COR10-1 (data not shown). EMT has previously been associated with EGFR TKI resistance in NSCLC (7, 25). In support of the results of the unsupervised analysis, comparison of

differentially expressed genes in the COR cell lines with the 76-gene EMT signature developed by Byers *et al*. (26) indicated a significant ($P < 0.0001$) overlap comparing the gene sets (SI Table 3A, B). In addition, parental and resistant clones are clustered into distinct groups using hierarchical clustering with the Byers' EMT gene signature (SI Fig. 9).

To confirm the differential expression of EMT markers identified by RNA-Seq, we analyzed COR-1 and COR10-1 CO-1686 resistant clones by qRT-PCR (Fig. 5C) and Western blot analysis (SI Fig. 10). Consistent with a mesenchymal cell signature in the COR clones, vimentin (*VIM*) expression was up-regulated and E-cadherin (*CDH1*) down-regulated in the CO-1686 resistant clones at the protein and RNA level. qRT-PCR analysis of additional markers further supported EMT including the up-regulation of *AXL*, *ZEB1, CDH5, FN1* and the down-regulation of the epithelial markers *MIR200B* (27), *CLDN4, EPCAM* and *CLDN7*. *EGFR* expression was moderately reduced in the COR cell clones compared to the parental NCI-H1975 cell line; however, *EGF* ligand expression was induced as demonstrated by qRT-PCR (Fig. 5C).

Amplification of the *MET* gene is observed in approximately 5-10% of NSCLC patients failing first generation EGFR TKIs (10, 28). An additional sub-population of EGFR TKI resistant patients also up-regulate the MET ligand, hepatocyte growth factor (HGF; (29)). Analysis of phosphorylated MET in the COR clones indicated that the HGF pathway was not activated following CO-1686 resistance in the NCI-H1975 cell line (SI Fig. 10), and expression of the *MET* receptor was significantly reduced in the COR cell clones at the RNA level (Fig. 5C). *ERBB2* amplification may be associated with acquired resistance especially in patients without detected T790M mutations (10, 30). Activation of additional EGFR receptor members ERBB2 and ERBB3 by phosphorylation was also not observed and actually appeared to be decreased in the COR clones compared to the parental NCI-H1975 cell line (Fig. 5C; SI Fig. 10).

CO-1686 resistant NSCLC cell lines are sensitive to AKT inhibition. We next examined potential druggable targets over-expressed in CO-1686 resistant cell clones that when inhibited could potentially restore CO-1686 sensitivity. Higher basal levels of phosphorylated AKT (pAKT) were observed in the COR cell clones compared to the parental NCI-H1975 cell line (SI Fig.10). Addition of CO-1686 resulted in the complete reduction of pAKT to negligible levels in the NCI-H1975 parental cell line (SI Fig. 10). In comparison, CO-1686 addition to the COR cell clones, while reducing pAKT did not completely inhibit pAKT levels (SI Fig. 10). Examining AKT isoform RNA expression in the COR cell clones by RNA-seq and qRT-PCR indicated that *AKT3* expression was up-regulated 12- and 121-fold, respectively ($P < 0.001$; Fig. 5C). Consistent with the RNA data, AKT3 was also up-regulated in the COR clones compared to the parental cell line at the protein level (SI Fig. 10). *AKT2* RNA was increased approximately 2-fold ($P < 0.001$) by RNA-Seq and qRT-PCR analysis (Fig. 5C). No change was observed for *AKT1* RNA expression (data not shown). Given the up-regulation of AKT isoforms and continued AKT signaling in the presence of CO-1686 in the COR cell clones, we examined the impact of AKT inhibition on CO-1686 resistance using the AKT inhibitors MK-2206 (31) and GDC-0068 (32) that are currently in clinical development for multiple oncology indications. Although not effective when used as a single agent (Fig. 5D), both MK-2206 and GDC-0068 restored partial drug sensitivity to the COR10-1 clone when used together in an equimolar fashion with CO-1686, with a combination index (CI) of 0.1, indicative of strong synergism. Synergy between AKT inhibition and CO-1686 was also observed in additional COR cell clones (data not shown).

The up-regulation of AXL receptor tyrosine kinase has previously been reported in EGFR-resistant NSCLC (25, 26). Consistent with these reports, AXL was observed to be up-regulated at the RNA (SI Table 2; Fig. 5C) and protein level (SI Fig. 10) in the CO-1686 resistant COR cell clones compared to the parental cell line. In addition, growth arrest-specific 6 (Gas6), a ligand of AXL implicated in EGFR TKI resistance (25, 33) was significantly up-regulated in COR cell clones as determined by RNA-Seq and qRT-PCR analysis (Fig. 5C). AXL kinase function was inhibited employing XL-880, a VEGFR/MET/AXL inhibitor (Foretinib; Exelixis (34)). Pharmacological inhibition of AXL kinase activity restored partial sensitivity of EGFR TKI resistant COR cell clones to CO-1686 (SI Fig. 11A), however, this effect was modest in comparison to previous reports (25) with a CI of 0.53 and 0.44 for COR1-1 and COR10-1, respectively, indicative of synergy. Combination of CO-1686 with R428, an AXL-selective small molecule inhibitor (35) produced comparable results to XL-880 (data not shown). Given the multiple targets inhibited by small molecule kinase inhibitors, the role of AXL inhibition in sensitizing COR cell clones to CO-1686 was specifically examined using siRNA to knockdown AXL expression (SI Fig.11B, C). Despite effective AXL knockdown at the mRNA and protein level (SI Fig. 11B) only a modest reduction in CO-1686 GI_{50} in the COR1-1 and COR10-1 clones of 2.2 and 1.6-fold, respectively (SI Fig. 11C), was observed. In addition, we generated stable pools of parental NCI-H1975 cells that over-expressed AXL at the mRNA and protein level (SI Fig. 11D) and determined the GI_{50} for CO-1686. Compared to the parental cell line, NCI-H1975 cell populations over-expressing AXL had a slight increase in CO-1686 GI_{50} of approximately 2-fold (SI Fig. 11E). To place this result into perspective, the CO-1686 GI_{50} of the COR cell clones 1-1 and 10-1 that over-express *AXL* ~100-fold over the parental NCI-H1975 cell line (Fig. 5C) are > 1000nM and the NCI-H1975 cell line engineered to over-express *AXL* at

195-fold above the parental cell line is 52 nM. Therefore, in our studies, although small molecule inhibitors of AXL kinase can partially restore the sensitivity of COR cell lines to CO-1686, the specific role of AXL inhibition in this effect appears minimal and perhaps related the broader spectrum of kinases inhibited by these agents.

DISCUSSION

T790M-driven lung cancer is a growing clinical problem given widespread screening of lung adenocarcinoma patients for activating EGFR mutations and consequent recommended use of erlotinib or gefitinib as front-line therapy in $EGFR^{mut}$ patients (NCCN guidelines version 2.2013 non-small cell lung cancer). Significantly, early clinical evidence suggests that a secondary T790M mutation can drive resistance to second generation TKIs such as afatinib as well (36). CO-1686 has attractive relevant properties as a potential therapeutic for T790M positive $EGFR^{mut}$ NSCLC. It potently inhibits the kinase activity of EGFR carrying the T790M mutation, both *in vitro* and after oral administration *in vivo* (cell line xenograft and patient-derived xenograft). This inhibitory activity against a pathogenic mutant form of EGFR is not accompanied by meaningful wild-type EGFR inhibition, suggesting that drug tolerability may be superior to first and second generation TKIs, for which key toxicities of skin rash, diarrhea and interstitial lung disease are attributed to wild-type EGFR inhibition (6, 37). CO-1686 is currently in a human dose-escalation study to evaluate safety, pharmacokinetics, and preliminary efficacy in previously treated $EGFR^{mut}$ NSCLC patients (ClinicalTrials.gov identifier: NCT01526928). Although still in dose-escalation phase and the maximal tolerated dose not reached, objective RECIST responses have been observed in heavily pretreated T790M positive NSCLC patients administered CO-1686 following the development of resistance to erlotinib (38). Additionally, metastasis shrinkage has been observed at multiple organ sites, including both brain and liver metastases. Consistent with the preclinical data presented in this paper, CO-1686 appears to be well-tolerated with no evidence of dose-related diarrhea or rash.

CO-1686 potently inhibits single activating mutant forms of EGFR, both *in vitro* and *in vivo* (cell line xenograft and human EGFR transgenic mouse models). Assuming that this non-

clinical activity translates into clinical efficacy in treatment naïve $EGFR^{mut}$ patients, an interesting question is whether the development of acquired resistance to CO-1686 will be slower than acquisition of resistance to first generation TKIs, such that progression-free survival with CO-1686 would be superior to erlotinib. Initial studies of *in vitro* resistance to CO-1686 demonstrate enrichment of an RNA-based signature associated with EMT. A similar signature has been observed in cell lines resistant to EGFR and PI3K/Akt inhibitors (26). In support of the CO-1686 resistance data performed in the NCI-H1975 cell background, we have also generated CO-1686 resistant clones of the HCC827 cell line (*EGFR* del19). EMT is also associated with resistance in these cell clones, with the down-regulation of E-cadherin and up-regulation of vimentin at the RNA and protein level (data not shown). In addition, recent work from two independent investigators using a tool-compound structurally related to CO-1686, termed CNX-2006 (Celgene), also indicated that EMT is associated with resistance in multiple cell backgrounds (39, 40). Recent papers indicate that resistance to WZ4002, a covalent EGFR inhibitor, is mediated by IGF1R pathway activation due to the repression of IGFBP3 expression via promoter methylation (41) or genomic amplification of the *MAPK1* (*ERK2*) gene (42). These specific mechanisms were not observed in our studies (data not shown). Two key next steps with CO-1686 are (a) to assess the kinetics of acquired EMT and compare with acquired T790M using *in vitro* and *in vivo* systems, and (b) to examine the value of combinatorial therapy targeting the specific resistance pathways defined above. It is encouraging that resistance to CO-1686 has not yet been observed to be driven by direct EGFR pathway modification. This suggests that CO-1686 may be sufficient to functionally silence mutant EGFR signaling at clinically achievable concentrations, a key therapeutic goal in $EGFR^{mut}$ NSCLC that has not been achieved with the currently available clinical TKIs due to acquired resistance within the pathway

that leads to patient relapse. Moreover, the sparing of wild-type EGFR by CO-1686 may allow for evaluation of combination therapies with less potential for overlapping toxicities in patients.

MATERIALS AND METHODS

Note that additional materials and methods are included in supplementary materials.

Cell culture. NCI-H1975, HCC827, HCC-H1299, NCI-H358 human NSCLC adenocarcinoma cells and A431 human epidermoid carcinoma were obtained from the American Type Culture Center (Manassas, VA). PC-9 cells were a kind gift of Dr. F. Koizumi (National Cancer Center Research Institute & Shien-Lab, Japan). HCC827-EPR cells (18) were a kind gift of Dr. S. Kenichi (Aichi Cancer Center Hospital, Japan). 293H cells were purchased from Invitrogen (Carlsbad, CA). PC-9/ER and H3255/XLR cells were derived in the Pao Lab (20). Cell line identity was confirmed by short tandem repeat (STR) analysis (Genetica, Burlington, NC) and cells used for no longer than 6 months before being replaced. NCI-H1975, HCC827, HCC-H1299, NCI-H358 and PC-9 cells were grown in RPMI 1640 (Life Technologies; Carlsbad, CA) supplemented with 10% FBS (HyClone; South Logan, UT), 2 mM L-glutamine, and 1% Penicillin-Streptomycin (Mediatech; Corning, NY). A431 cells were grown in DMEM (Life Technologies; Carlsbad, CA) supplemented with 10% FBS (HyClone), 2 mM L-glutamine, and 1% Penicillin-Streptomycin (Mediatech). HCC827-EPR cells were grown in RPMI 1640 supplemented with 10 % FBS, 2 mM L-glutamine, 1 % Penicillin-Streptomycin, 1 μM erlotinib, and 1 μM PHA-665752 (Selleck Chemical, Houston, TX). PC-9/ER and H3255/XLR cells were grown in the same media as above supplemented with 1 μM erlotinib (Selleck). All cells were maintained and propagated as monolayer cultures at 37^{o}C in a humidified 5% CO_2 incubator.

Cell proliferation assays. Cells were seeded at 3,000 cells/well in growth media supplemented with 5% FBS, 2 mM L-glutamine, and 1 % P/S, allowed to adhere overnight, and treated with a dilution series of test compound for 72 hr. Cell viability was determined by CellTiter Glo

(Promega; Madison, WI) and results were represented as background-subtracted relative light units normalized to a DMSO-treated control. Growth inhibition (GI_{50}) values were determined by GraphPad Prism 5.04 (GraphPad Software; La Jolla, CA). MK-2206 and XL-880 compounds were obtained from Selleck Chemical (Houston, TX). Combination index (CI) data was generated using CalcuSyn (Biosoft, Ferguson MO).

Cell signaling analysis of HCC827 and HCC827-EPR. HCC827 and HCC827-EPR cells were seeded at $1.5x10^6$ cells per 10 cm^2 dish in RPMI 1640, 10 % FBS, 2 mM L-glutamine, and 1% P/S and allowed to adhere overnight. Cells were treated with DMSO, 2 μM CO-1686, or 2 μM erlotinib for 72 hours and lysed. Lysis buffer contained 1X phenylmethanesulfonyl fluoride (Sigma; St. Louis, MO), 1X cell extraction buffer (Life Technologies), 1X protease inhibitor cocktail (Enzo Life Sciences; Farmingdale, NY), 1X phosphatase inhibitor cocktails I and II (EMD Chemicals; Gibbstown, NJ). Total protein concentration was determined using a standard Bradford and measured on a NanoDrop 2000 spectrophotometer (Thermo Scientific; Waltham, MA). Western blotting was performed on cell lysates normalized to 25 μg total protein in loading buffer (LI-COR; Lincoln, NE). Normalized lysates were run on SDS/PAGE and transferred to a nitrocellulose membrane (Life Technologies). The membrane was incubated in Qentix signal enhancement solution (Thermo Scientific), blocked, and incubated overnight at 4°C with primary antibodies (1:1000) from Cell Signaling (Danvers, MA). Membranes were washed, incubated with IRDye® secondary antibodies (LI-COR), washed again, and imaged on an Odyssey Fc (LI-COR).

Analysis of minor EGFR mutations. 293H cells were transiently transfected with various pcDNA3.1(-) vectors using Lipofectamine 2000 (Invitrogen) and 2 μg DNA per sample as previous described (43). The EGFR G719S, ex19ins, ex20ins, T790M, and L858R + T790M mutations were all generated via site-directed mutagenesis as described (43). Following 6 hour treatment with DMSO, afatinib, or increasing doses of erlotinib or CO-1686 at various concentrations, cells were lysed. Immunoblotting was performed using corresponding lysates with antibodies against phospho-EGFR (Santa Cruz, Dallas, TX) or total EGFR (BD Biosciences, San Diego, CA). Secondary anti-goat antibody was obtained from Santa Cruz (Dallas, TX), and secondary anti-mouse antibody was obtained from Cell Signaling (Danvers, MA).

Xenograft studies. All the procedures related to animal handling, care, and the treatment in this manuscript were performed according to the guidelines approved by Institutional Animal Care and Use Committees (IACUC) following the guidance of the Association for Assessment and Accreditation of Laboratory Animal Care (AAALAC). Cell line xenograft studies (NCI-H1975, HCC827 and A431) were performed by Charles River Laboratories (Wilmington, MA). Briefly, NCr nu/nu mice were sub-cutaneously implanted with $1x10^7$ tumor cells in 50% Matrigel (injection volume of 0.2 mL/mouse). Once tumors reached 100-200 mm^3, Animals were dosed with compounds as outlined (N=10 animals/gp). The LUM1686 PDX xenograft study was performed by CrownBio (Santa Clara, CA). Briefly, LUM1686 PDX tumor fragments, harvested from donor mice, were inoculated into BALB/c nude mice. Administration of test compounds was initiated at a mean tumor size of approximately 160 mm^3. Tumor growth was monitored over time to determine tumor growth inhibition of the experimental agent vs. vehicle. The

endpoint of the experiment was a mean tumor volume (MTV) in control group of 2000 mm^3. Percent TGI was defined as the difference between the MTV of the designated control group and the MTV of the drug-treated group, expressed as a percentage of the MTV of the designated control group. The mean tumor volume in the treatment group(s) versus control group was compared using either Student's *t*-test for studies with only two groups or analysis of variance (ANOVA) followed by Tukey's test for studies with more than two groups. Data is presented as mean ± standard error of the mean (SEM).

Immunohistochemistry of skin tissues. Phospho-p44/42 mitogen activated protein kinase (MAPK; Erk1/2, Thr202/Tyr204, Rabbit mAb) was purchased from Cell Signaling Technology. Peroxidase-based immunohistochemistry detection system (EnVision+ System-HRP, Rabbit (DAB+)), antibody diluent, and serum-free protein block were purchased from Dako (Carpinteria, CA). Formalin-fixed paraffin-embedded tissue skin sections underwent antigen retrieval, endogenous peroxidase block and were incubated with primary antibody overnight at 4^oC. Following overnight incubation, slides were rinsed in washed and incubated a peroxidase-labeled polymer. The tissue sections were then rinsed and stained with 3,3'-Diaminobenzidine (DAB) substrate-chromogen and then counterstained with Hematoxylin Gill I (EMD Millipore) and bluing reagent (EMD Millipore). Electronic images were captured using Leica DM1000 LED microscope (40x objective) with Leica DFC295 camera and Leica Application Suite (Leica Microsystems, Buffalo Grove, IL).

EGFR-L858R and EGFR-L858R-T790M;CCSP-rtTA transgenic mouse models. Bitransgenic EGFR mutant;CCSP-rtTA mice were housed and cared for at NCI-Frederick

facilities. NCI-Frederick is accredited by AAALAC International and follows the Public Health Service Policy for the Care and Use of Laboratory Animals. Animal care was provided in accordance with the procedures outlined in the "Guide for Care and Use of Laboratory Animals" (National Research Council; 1996; National Academy Press; Washington, D.C.). All the studies were conducted according to an approved Animal Care and Use Committee protocol. CCSP-rtTA transgenic mice were purchased from the Jackson Laboratory (www.jax.org) and crossed to Tet-op-EGFR-L858R transgenic mice obtained from the NCI mouse repository (http://mouse.ncifcrf.gov/), or to Tet-op-EGFR-L858R-T790M mice obtained from Dr. Kwok-Kin Wong (Dana-Farber Cancer Institute). Detection of the CCSP-rtTA, Tet-op-L858R and Tet-op-EGFR-L858R-T790M alleles was performed as described previously (23, 24). Mice were given doxycycline feed to induce lung tumorigenesis at 9-10 weeks of age. After 4 weeks of induction, mice were imaged by MR for baseline tumor measurements, and were recruited into drug treatment groups. Mouse lungs were imaged with a Philips Intera Achieva 3.0T MRI clinical scanner. Three dimensional volume image analysis was performed using ITK-SNAP software from the Penn Image Computing and Science Laboratory (University of Pennsylvania). Erlotinib (LC Laboratories) was resuspended in 0.5%methycellulose / 0.4% Tween 80 to a concentration of 5.0 mg/ml and dosed daily by oral gavage at 10 ml/kg for a final dose of 50 mg/kg. Afatinib (Chemietek) was resuspended in 0.5 % methylcellulose/0.4% Tween 80 to a concentration of 2.0 mg/ml and dosed daily by oral gavage at 10ml/kg for a final dose of 20 mg/kg. O-1686 was resuspended in warmed DMSO:Solutol HS15: PBS (5:15:80; v:v:v) and dosed twice daily (BID) by oral gavage at 10ml/kg for a final dose of 50 mg/kg. Body weights were taken twice weekly and used to calculate dose volumes for subsequent days.

REFERENCES

1. Herbst RS, Heymach JV, Lippman SM. Lung cancer. N Engl J Med. 2008;359:1367-80.
2. Rosell R, Moran T, Queralt C, Porta R, Cardenal F, Camps C, et al. Screening for epidermal growth factor receptor mutations in lung cancer. N Engl J Med. 2009;361:958-67.
3. Mok TS, Wu YL, Thongprasert S, Yang CH, Chu DT, Saijo N, et al. Gefitinib or carboplatin-paclitaxel in pulmonary adenocarcinoma. N Engl J Med. 2009;361:947-57.
4. Fukuoka M, Wu YL, Thongprasert S, Sunpaweravong P, Leong SS, Sriuranpong V, et al. Biomarker analyses and final overall survival results from a phase III, randomized, open-label, first-line study of gefitinib versus carboplatin/paclitaxel in clinically selected patients with advanced non-small-cell lung cancer in Asia (IPASS). J Clin Oncol. 2011;29:2866-74.
5. Rosell R, Carcereny E, Gervais R, Vergnenegre A, Massuti B, Felip E, et al. Erlotinib versus standard chemotherapy as first-line treatment for European patients with advanced EGFR mutation-positive non-small-cell lung cancer (EURTAC): a multicentre, open-label, randomised phase 3 trial. Lancet Oncol. 2012;13:239-46.
6. Herbst RS, LoRusso PM, Purdom M, Ward D. Dermatologic side effects associated with gefitinib therapy: clinical experience and management. Clin Lung Cancer. 2003;4:366-9.
7. Sequist LV, Waltman BA, Dias-Santagata D, Digumarthy S, Turke AB, Fidias P, et al. Genotypic and histological evolution of lung cancers acquiring resistance to EGFR inhibitors. Sci Transl Med. 2011;3:75ra26.
8. Pao W, Miller VA, Politi KA, Riely GJ, Somwar R, Zakowski MF, et al. Acquired resistance of lung adenocarcinomas to gefitinib or erlotinib is associated with a second mutation in the EGFR kinase domain. PLoS Med. 2005;2:e73.
9. Sharma SV, Bell DW, Settleman J, Haber DA. Epidermal growth factor receptor mutations in lung cancer. Nat Rev Cancer. 2007;7:169-81.
10. Yu HA, Arcila ME, Rekhtman N, Sima CS, Zakowski MF, Pao W, et al. Analysis of Tumor Specimens at the Time of Acquired Resistance to EGFR-TKI Therapy in 155 Patients with EGFR-Mutant Lung Cancers. Clin Cancer Res. 2013.
11. Kwak EL, Sordella R, Bell DW, Godin-Heymann N, Okimoto RA, Brannigan BW, et al. Irreversible inhibitors of the EGF receptor may circumvent acquired resistance to gefitinib. Proc Natl Acad Sci U S A. 2005;102:7665-70.
12. Kobayashi S, Boggon TJ, Dayaram T, Jänne PA, Kocher O, Meyerson M, et al. EGFR mutation and resistance of non-small-cell lung cancer to gefitinib. N Engl J Med. 2005;352:786-92.
13. Yun CH, Mengwasser KE, Toms AV, Woo MS, Greulich H, Wong KK, et al. The T790M mutation in EGFR kinase causes drug resistance by increasing the affinity for ATP. Proc Natl Acad Sci U S A. 2008;105:2070-5.
14. Miller VA, Hirsh V, Cadranel J, Chen YM, Park K, Kim SW, et al. Afatinib versus placebo for patients with advanced, metastatic non-small-cell lung cancer after failure of erlotinib, gefitinib, or both, and one or two lines of chemotherapy (LUX-Lung 1): a phase 2b/3 randomised trial. Lancet Oncol. 2012;13:528-38.
15. Zhou W, Ercan D, Chen L, Yun CH, Li D, Capelletti M, et al. Novel mutant-selective EGFR kinase inhibitors against EGFR T790M. Nature. 2009;462:1070-4.
16. Lee HJ, Schaefer G, Heffron TP, Shao L, Ye X, Sideris S, et al. Noncovalent wild-type-sparing inhibitors of EGFR T790M. Cancer Discov. 2013;3:168-81.

17. Karaman MW, Herrgard S, Treiber DK, Gallant P, Atteridge CE, Campbell BT, et al. A quantitative analysis of kinase inhibitor selectivity. Nat Biotechnol. 2008;26:127-32.
18. Suda K, Murakami I, Katayama T, Tomizawa K, Osada H, Sekido Y, et al. Reciprocal and complementary role of MET amplification and EGFR T790M mutation in acquired resistance to kinase inhibitors in lung cancer. Clin Cancer Res. 2010;16:5489-98.
19. Van de Vijver MJ, Kumar R, Mendelsohn J. Ligand-induced activation of A431 cell epidermal growth factor receptors occurs primarily by an autocrine pathway that acts upon receptors on the surface rather than intracellularly. J Biol Chem. 1991;266:7503-8.
20. Chmielecki J, Foo J, Oxnard GR, Hutchinson K, Ohashi K, Somwar R, et al. Optimization of dosing for EGFR-mutant non-small cell lung cancer with evolutionary cancer modeling. Sci Transl Med. 2011;3:90ra59.
21. Ohashi K, Maruvka YE, Michor F, Pao W. Epidermal growth factor receptor tyrosine kinase inhibitor-resistant disease. J Clin Oncol. 2013;31:1070-80.
22. Merlino GT, Xu YH, Ishii S, Clark AJ, Semba K, Toyoshima K, et al. Amplification and enhanced expression of the epidermal growth factor receptor gene in A431 human carcinoma cells. Science. 1984;224:417-9.
23. Politi K, Zakowski MF, Fan PD, Schonfeld EA, Pao W, Varmus HE. Lung adenocarcinomas induced in mice by mutant EGF receptors found in human lung cancers respond to a tyrosine kinase inhibitor or to down-regulation of the receptors. Genes Dev. 2006;20:1496-510.
24. Li D, Shimamura T, Ji H, Chen L, Haringsma HJ, McNamara K, et al. Bronchial and peripheral murine lung carcinomas induced by T790M-L858R mutant EGFR respond to HKI-272 and rapamycin combination therapy. Cancer Cell. 2007;12:81-93.
25. Zhang Z, Lee JC, Lin L, Olivas V, Au V, LaFramboise T, et al. Activation of the AXL kinase causes resistance to EGFR-targeted therapy in lung cancer. Nat Genet. 2012;44:852-60.
26. Byers LA, Diao L, Wang J, Saintigny P, Girard L, Peyton M, et al. An epithelial-mesenchymal transition gene signature predicts resistance to EGFR and PI3K inhibitors and identifies Axl as a therapeutic target for overcoming EGFR inhibitor resistance. Clin Cancer Res. 2013;19:279-90.
27. Burk U, Schubert J, Wellner U, Schmalhofer O, Vincan E, Spaderna S, et al. A reciprocal repression between ZEB1 and members of the miR-200 family promotes EMT and invasion in cancer cells. EMBO Rep. 2008;9:582-9.
28. Engelman JA, Zejnullahu K, Mitsudomi T, Song Y, Hyland C, Park JO, et al. MET amplification leads to gefitinib resistance in lung cancer by activating ERBB3 signaling. Science. 2007;316:1039-43.
29. Yano S, Wang W, Li Q, Matsumoto K, Sakurama H, Nakamura T, et al. Hepatocyte growth factor induces gefitinib resistance of lung adenocarcinoma with epidermal growth factor receptor-activating mutations. Cancer Res. 2008;68:9479-87.
30. Takezawa K, Pirazzoli V, Arcila ME, Nebhan CA, Song X, de Stanchina E, et al. HER2 amplification: a potential mechanism of acquired resistance to EGFR inhibition in EGFR-mutant lung cancers that lack the second-site EGFRT790M mutation. Cancer Discov. 2012;2:922-33.
31. Hirai H, Sootome H, Nakatsuru Y, Miyama K, Taguchi S, Tsujioka K, et al. MK-2206, an allosteric Akt inhibitor, enhances antitumor efficacy by standard chemotherapeutic agents or molecular targeted drugs in vitro and in vivo. Mol Cancer Ther. 2010;9:1956-67.

32. Blake JF, Xu R, Bencsik JR, Xiao D, Kallan NC, Schlachter S, et al. Discovery and preclinical pharmacology of a selective ATP-competitive Akt inhibitor (GDC-0068) for the treatment of human tumors. J Med Chem. 2012;55:8110-27.
33. Stitt TN, Conn G, Gore M, Lai C, Bruno J, Radziejewski C, et al. The anticoagulation factor protein S and its relative, Gas6, are ligands for the Tyro 3/Axl family of receptor tyrosine kinases. Cell. 1995;80:661-70.
34. Liu L, Greger J, Shi H, Liu Y, Greshock J, Annan R, et al. Novel mechanism of lapatinib resistance in HER2-positive breast tumor cells: activation of AXL. Cancer Res. 2009;69:6871-8.
35. Holland SJ, Pan A, Franci C, Hu Y, Chang B, Li W, et al. R428, a selective small molecule inhibitor of Axl kinase, blocks tumor spread and prolongs survival in models of metastatic breast cancer. Cancer Res. 2010;70:1544-54.
36. Kim Y, Ko J, Cui Z, Abolhoda A, Ahn JS, Ou SH, et al. The EGFR T790M mutation in acquired resistance to an irreversible second-generation EGFR inhibitor. Mol Cancer Ther. 2012;11:784-91.
37. Camus P, Kudoh S, Ebina M. Interstitial lung disease associated with drug therapy. Br J Cancer. 2004;91 Suppl 2:S18-23.
38. Sequist LV, Soria J-C, Gadgeel SM, Wakelee HA, Camidge DR, Varga A, et al. First-in-human evaluation of CO-1686, an irreversible, selective, and potent tyrosine kinase inhibitor of EGFR T790M. American Society of Clinical Oncology; 2013; Chicago, IL: Journal of Clinical Oncology.
39. Ohashi K, Suda K, Sun J, Pan Y, Walter A, Haringsma H, et al. CNX-2006, a novel irreversible epidermal growth factor receptor (EGFR) inhibitor, selectively inhibits EGFR T790M and fails to induce T790M-mediated resistance in vitro. American Association of Cancer Research; 2013; Washington, DC.
40. Galvani E, Giovannetti E, Walter A, Haringsma H, Tjin R, Dekker H, et al. Role of epithelial-mesenchymal transition (EMT) in sensitivity to CNX-2006, a novel mutant-selective EGFR inhibitor with overcomes in vitro T790M-mediated resistance in NSCLC. American Association of Cancer Research; 2013; Washington, DC.
41. Cortot AB, Repellin CE, Shimamura T, Capelletti M, Zejnullahu K, Ercan D, et al. Resistance to irreversible EGF receptor tyrosine kinase inhibitors through a multistep mechanism involving the IGF1R pathway. Cancer Res. 2013;73:834-43.
42. Ercan D, Xu C, Yanagita M, Monast CS, Pratilas CA, Montero J, et al. Reactivation of ERK signaling causes resistance to EGFR kinase inhibitors. Cancer Discov. 2012;2:934-47.
43. Pao W, Miller V, Zakowski M, Doherty J, Politi K, Sarkaria I, et al. EGF receptor gene mutations are common in lung cancers from "never smokers" and are associated with sensitivity of tumors to gefitinib and erlotinib. Proc Natl Acad Sci U S A. 2004;101:13306-11.

Table 1: Kinetic parameters of EGFR inhibition by CO-1686

Compounds	Parameters	$EGFR^{L858R/T790M}$	$EGFR^{WT}$	Ratio*
CO-1686	K_I (nM)	21.5 ± 1.7	303.3 ± 26.7	14.1
	k_{inact} (s^{-1})	0.0051 ± 0.0003	0.0034 ± 0.0005	NA
	k_{inact}/K_I ($M^{-1} s^{-1}$)	(2.41 ± 0.30) x 10^5	(1.12 ± 0.14) x 10^4	21.51
Erlotinib	K_I (nM)	98.0 ± 8.1	0.40 ± 0.03	0.0041

*Ratio determined by $EGFR^{WT}$ / $EGFR^{L858R/T790M}$

NA: Not applicable

Table 2: Sensitivity of CO-1686 resistant NCI-1975 cell clones to EGFR TKIs

Cell line	CO-1686 GI_{50} (nM)	Erlotinib GI_{50} (nM)	Afatinib GI_{50} (nM)
NCI-H1975	9±5	2227±1326	36±25
COR 1-1	3237±1114	>5000	3114±922
COR 1-2	1700±64	>5000	1817
COR 10-1	2964±1280	>5000	3197
COR 10-2	>4582	>5000	3866
COR 10-3	3815±735	>5000	2588

FIGURE LEGENDS

Figure 1. (A) Chemical structure of CO-1686. Reactive acrylamide group is highlighted by dashed circle. (B) Structural modeling of CO-1686 binding to T790M EGFR. The EGFR T790M kinase is shown in a ribbon representation (green) with the bound CO-1686 in orange. The aminopyrimidine binds to the hinge residues Met793 through hydrogen bonding (yellow dashed lines). The C5-CF3 substitution points to the gatekeeper residue Met790. Both C2 and C4 substitutions adapt a U-shaped binding mode. The piperazine ring is facing an open space in the solvent exposure area. The *meta* acrylamide points to Cys797 and forms the covalent bond.

Figure 2. (A) CO-1686 inhibits viability in EGFR-mutant cell lines *in vitro*. The CO-1686 GI_{50} was determined in cells harboring mutant or WT EGFR. Cell viability was analyzed using the CellTiter-Glo viability assay. GI_{50} values shown on Log10 scale in nM as an average of 3 or more independent experiments ± SEM. (B) CO-1686 induces apoptosis in parental HCC827 (EGFR del19) as well as erlotinib-resistant HCC827-EPR cells (EGFR del19/T790M). Levels of cleaved PARP (CI-PARP), Bim-EL, phosphorylated EGFR (pEGFR), phosphorylated MAPK (pMAPK) and phosphorylated ribosomal protein S6 (pS6RP) were determined after 72 hours treatment with CO-1686 or erlotinib in HCC827 cells expressing EGFRdel19 +/- T790M.

Figure 3. *In vivo* antitumor efficacy of CO-1686 in lung (A) NCI-H1975, (B) LUM1868, (C) HCC827 and (D) squamous epidermoid A431 xenograft models. CO-1686 was administered orally (PO), daily (QD) or twice daily (BID) at concentrations ranging from 3, 10, 30 and 100 mg/kg/day. N=10 animals/gp. Data plotted as mean ± SEM.

Figure 4. CO-1686 does not inhibit WT EGFR signaling *in vivo* and is active in EGFR-mutant transgenic mouse lung cancer models. (A, B) EGFR signaling was examined in A431 (WT EGFR) tumors following CO-1686 (50 mg/kg BID, PO), erlotinib (75 mg/kg QD, PO) or afatinib (20 mg/kg QD, IP) administration (N=4 animals/gp). Established (80-120 mm^3) A431 tumors following five days of drug administration were harvested at 4 hours post-last dose for tumor WT EGFR signaling analysis. (A) Western blot of tumor lysates analyzed for phosphorylated EGFR (pEGFR) and downstream signaling analysis. (B) Quantification of pEGFR levels in A431 tumors. pEGFR levels from (A) were quantified by densitometry and plotted relative to the vehicle treated group (vehicle = 100%). Data plotted as mean ± SEM. * indicates $P < 0.05$ and ** $P < 0.005$ comparing vehicle to treated groups. (C) WT EGFR signaling in mouse skin is not affected by CO-1686. Representative immunohistochemical pMAPK staining in normal skin from mice administered with vehicle, CO-1686 (100 mg/kg QD, PO), afatinib (20 mg/kg QD, IP) or erlotinib (100 mg/kg QD, PO). Arrow indicates pMAPK positive nuclear staining in vehicle and CO-1686 groups (20X magnification). (D and E) *In vivo* antitumor activity of CO-1686 in $EGFR^{L858R}$ and $EGFR^{L858R/T790M}$ GEM models. Representative lung MRI images of mice treated with the indicated compound are shown (* in MRI image indicates a region of tumor formation). The bar graph shows lung tumor volume measurements (mean ± SEM) at baseline and following 21-days of dosing with the indicated compounds. * indicates $P < 0.05$ and ** indicates $P < 0.001$ comparing vehicle and indicated groups 21-days post-dosing.

Figure 5. (A, B) CO-1686 resistant NCI-H1975 cell clones, COR1-1 and COR10-1 display a reduced dependence on EGFR signaling for survival. (A) Effect of EGFR siRNA transfection on EGFR protein expression in CO-1686 resistant clones (COR 1-1 and COR 10-1) and NCI-H1975 parental as determined Western blotting. (B) Impact of EGFR siRNA knock-down on cell viability in NCI-H1975, COR1-1 and COR10-1 clones. Cell viability was determined 72-hours post-siRNA transfection and plotted relative to the siRNA control treated group (representing 100%). Data plotted as mean ± SEM. * indicates $P < 0.05$ and ** $P < 0.005$ comparing siCTRL and siEGFR groups. (C) qRT-PCR analysis of EMT-related and EGFR-related genes in COR1-1 and COR10-1 cell clones. Data plotted as fold change relative to parental NCI-H1975 cells ± SEM. All data shown $P < 0.05$ comparing COR clone to parental. (D) Inhibition of AKT restores partial sensitivity of COR cell clones to CO-1686. COR10-1 was exposed to CO-1686, the AKT-inhibitors MK-2206 (left panel) or GDC-0068 (right panel), or an equimolar combination of AKT inhibitor + CO-1686. 72 hours post-drug addition cell viability was determined by CellTiterGlo. Data plotted as % viability relative to DMSO (no drug) control.

Figure 1

A

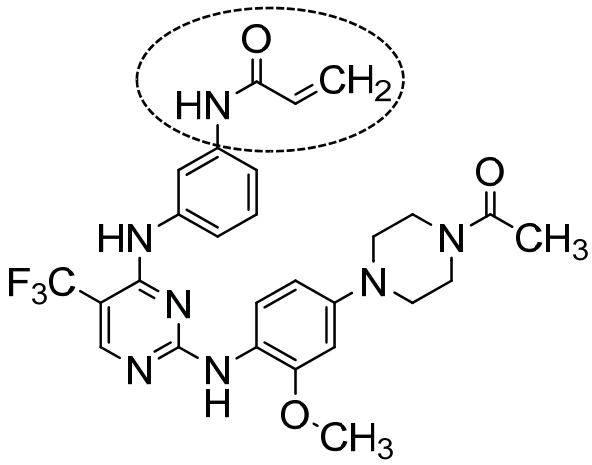

CO-1686

B

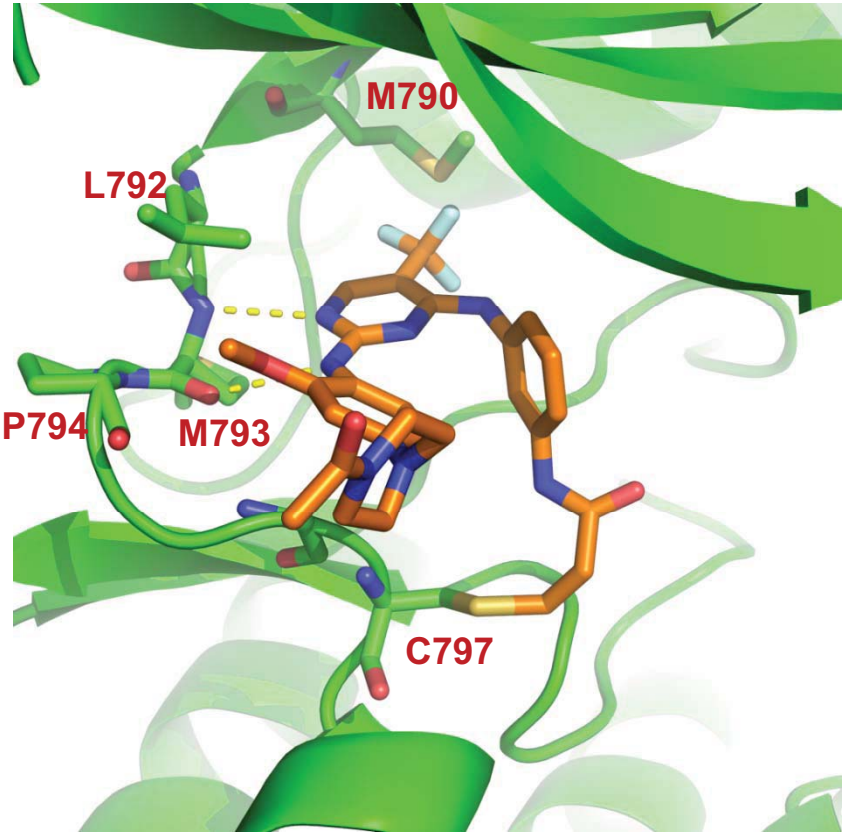

Figure 2

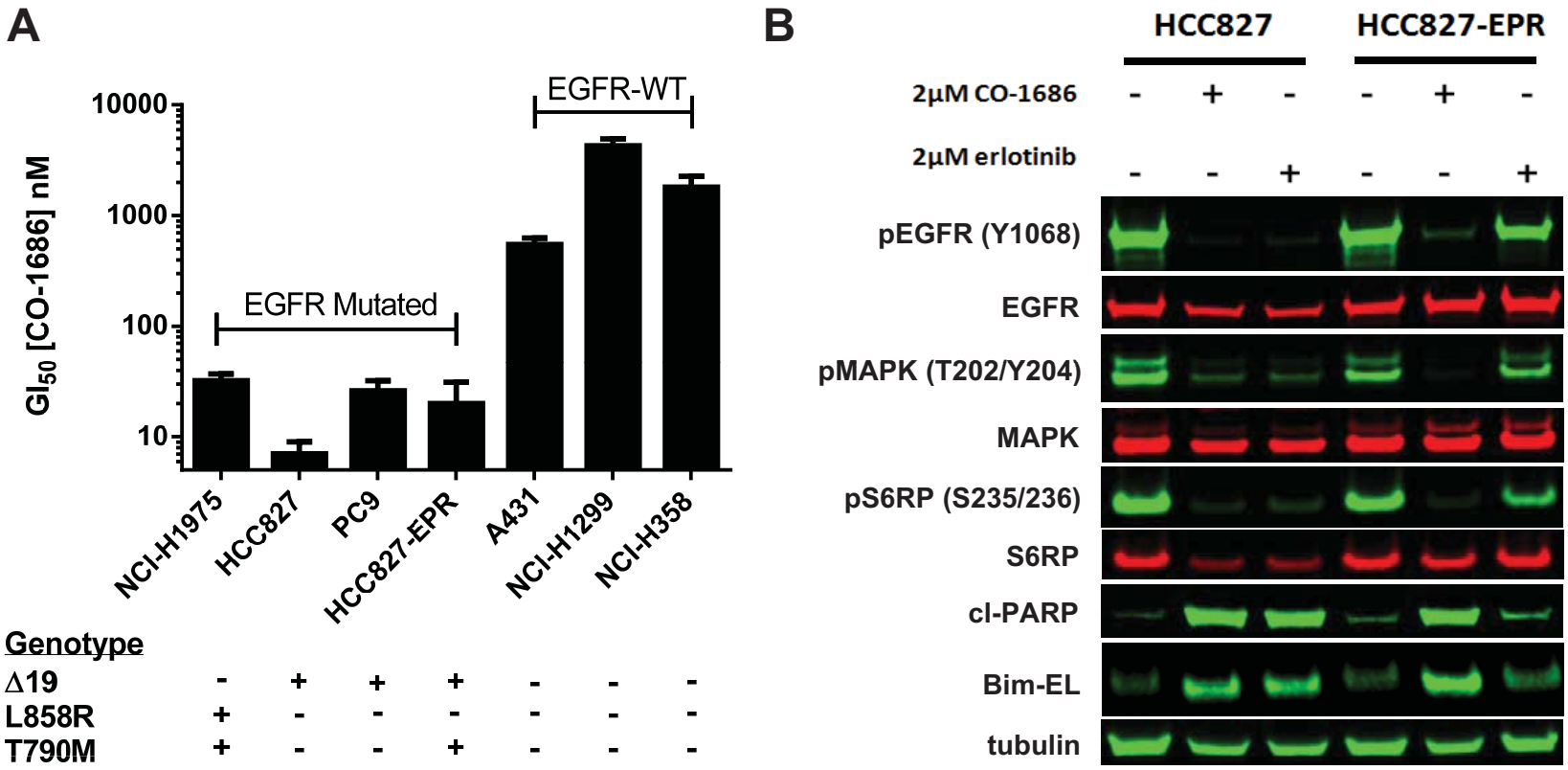
A
EGFR-WT
EGFR Mutated
10000
1000
100
10
GI50 [CO-1686] nM
NCI-H1975
HCC827
PC9
HCC827-EPR
A431
NCI-H1299
NCI-H358
Genotype
Δ19 - + + + - - -
L858R + - - - - - -
T790M + - - + - - -
B
HCC827
HCC827-EPR
2μM CO-1686 - + - - + -
2μM erlotinib - - + - - +
pEGFR (Y1068)
EGFR
pMAPK (T202/Y204)
MAPK
pS6RP (S235/236)
S6RP
cl-PARP
Bim-EL
tubulin

Figure 3

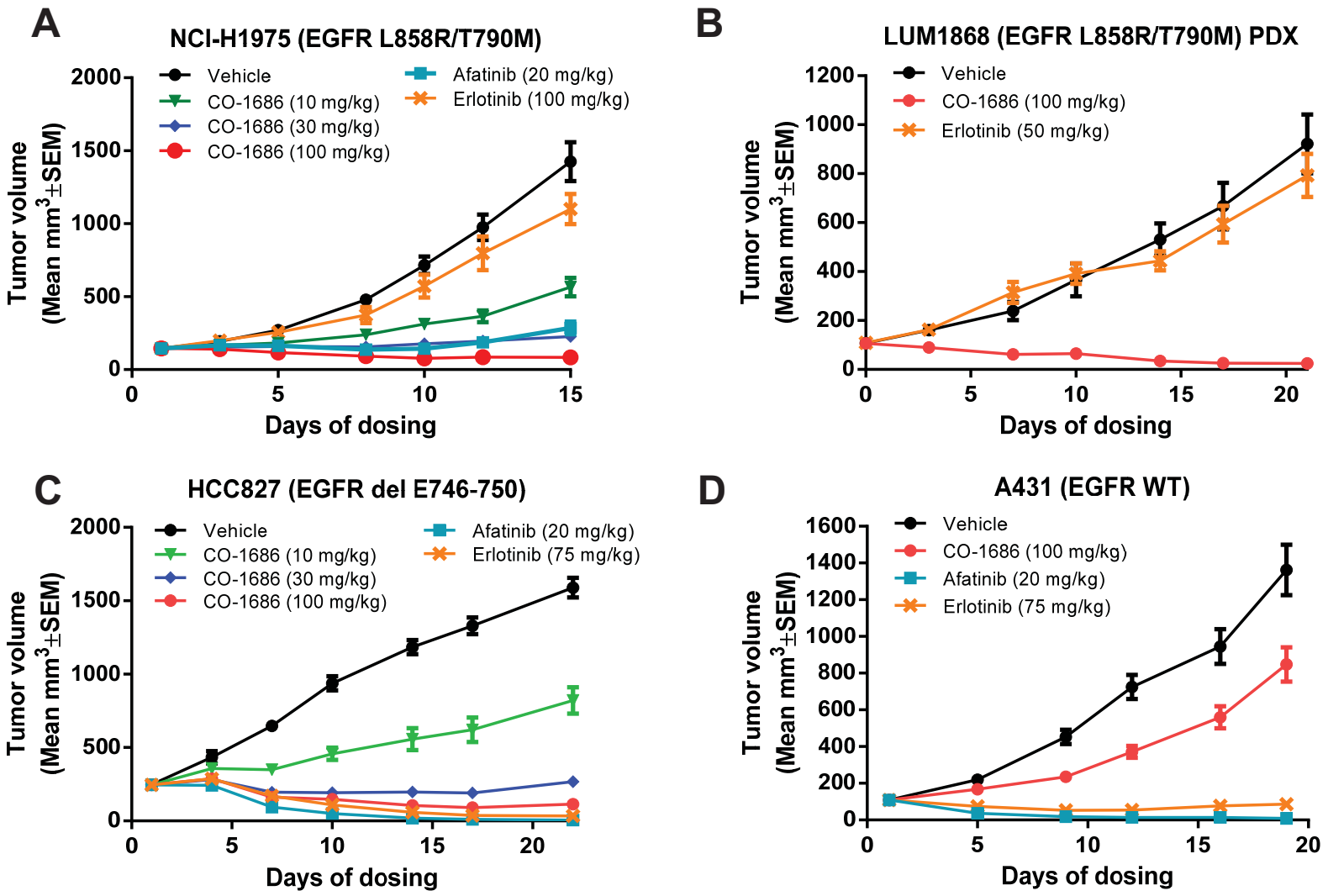
A
NCI-H1975 (EGFR L858R/T790M)
Vehicle
CO-1686 (10 mg/kg)
CO-1686 (30 mg/kg)
CO-1686 (100 mg/kg)
Afatinib (20 mg/kg)
Erlotinib (100 mg/kg)
Tumor volume (Mean mm3±SEM)
Days of dosing
B
LUM1868 (EGFR L858R/T790M) PDX
Vehicle
CO-1686 (100 mg/kg)
Erlotinib (50 mg/kg)
Tumor volume (Mean mm3±SEM)
Days of dosing
C
HCC827 (EGFR del E746-750)
Vehicle
CO-1686 (10 mg/kg)
CO-1686 (30 mg/kg)
CO-1686 (100 mg/kg)
Afatinib (20 mg/kg)
Erlotinib (75 mg/kg)
Tumor volume (Mean mm3±SEM)
Days of dosing
D
A431 (EGFR WT)
Vehicle
CO-1686 (100 mg/kg)
Afatinib (20 mg/kg)
Erlotinib (75 mg/kg)
Tumor volume (Mean mm3±SEM)
Days of dosing

Figure 4

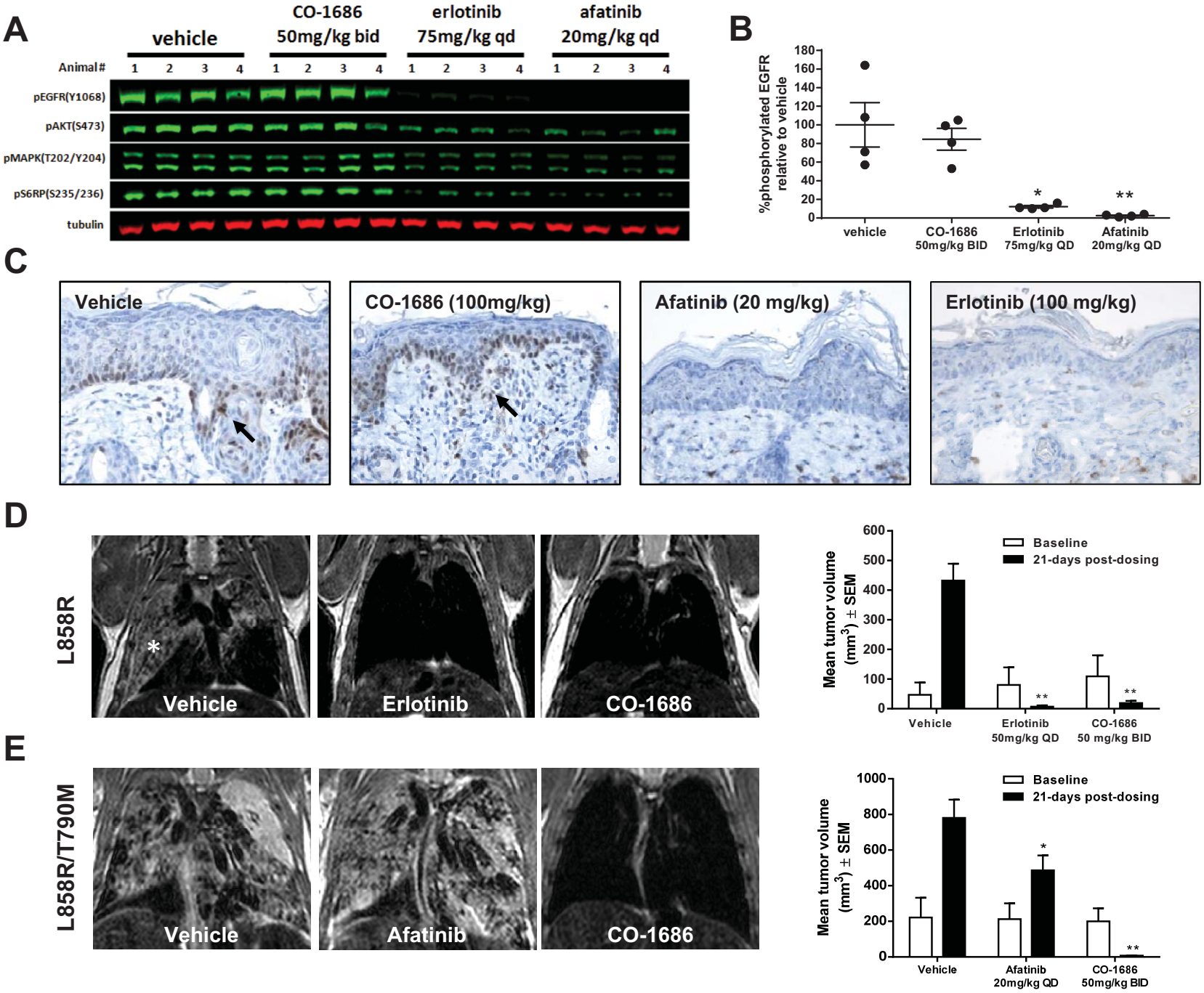
A
vehicle
CO-1686 50mg/kg bid
erlotinib 75mg/kg qd
afatinib 20mg/kg qd
Animal #
1 2 3 4 1 2 3 4 1 2 3 4 1 2 3 4
pEGFR(Y1068)
pAKT(S473)
pMAPK(T202/Y204)
pS6RP(S235/236)
tubulin
B
%phosphorylated EGFR relative to vehicle
vehicle
CO-1686 50mg/kg BID
Erlotinib 75mg/kg QD
Afatinib 20mg/kg QD
C
Vehicle
CO-1686 (100mg/kg)
Afatinib (20 mg/kg)
Erlotinib (100 mg/kg)
D
L858R
Vehicle
Erlotinib
CO-1686
Mean tumor volume (mm3) ± SEM
Baseline
21-days post-dosing
Vehicle
Erlotinib 50mg/kg QD
CO-1686 50 mg/kg BID
E
L858R/T790M
Vehicle
Afatinib
CO-1686
Mean tumor volume (mm3) ± SEM
Baseline
21-days post-dosing
Vehicle
Afatinib 20mg/kg QD
CO-1686 50mg/kg BID

Figure 5

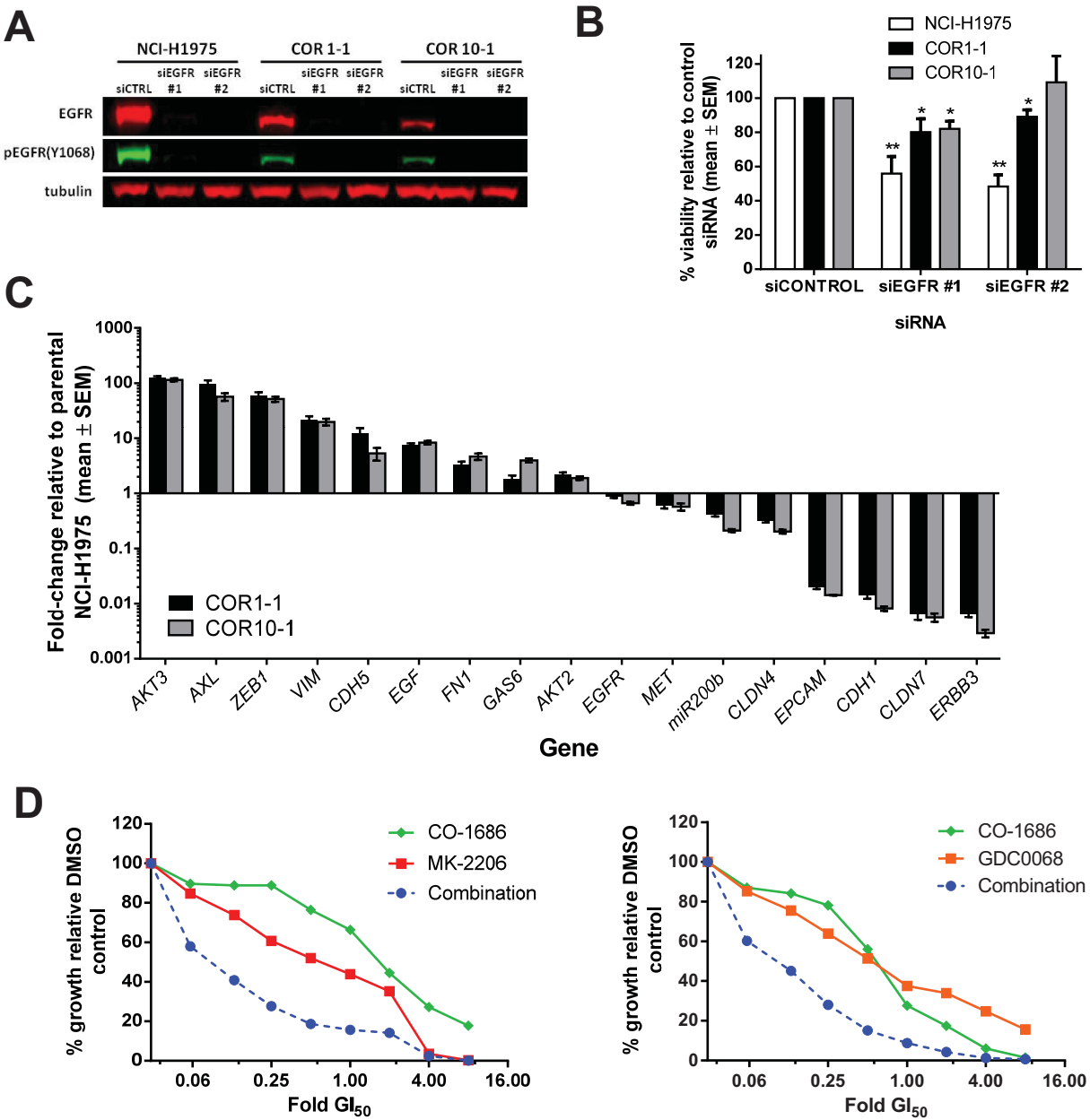
A
NCI-H1975
COR 1-1
COR 10-1
siCTRL
siEGFR #1
siEGFR #2
EGFR
pEGFR(Y1068)
tubulin
B
NCI-H1975
COR1-1
COR10-1
% viability relative to control siRNA (mean ± SEM)
siCONTROL
siEGFR #1
siEGFR #2
siRNA
C
Fold-change relative to parental NCI-H1975 (mean ± SEM)
COR1-1
COR10-1
AKT3
AXL
ZEB1
VIM
CDH5
EGF
FN1
GAS6
AKT2
EGFR
MET
miR200b
CLDN4
EPCAM
CDH1
CLDN7
ERBB3
Gene
D
% growth relative DMSO control
CO-1686
MK-2206
Combination
Fold GI50
CO-1686
GDC0068
Combination
Fold GI50